NANO LETTERS

2004
Vol. 4, No. 4
613−617

Nanoscale Structural and Mechanical Characterization of a Natural Nanocomposite Material: The Shell of Red Abalone

Xiaodong Li,*,† Wei-Che Chang,†,‡ Yuh J. Chao,† Rizhi Wang,§ and Ming Chang‡

Department of Mechanical Engineering, University of South Carolina, 300 Main Street, Columbia, South Carolina 29208, Department of Mechanical Engineering, Chung Yuan Christian University, 22 Pu-Jen, Pu−Chung Li, Chung-Li (32023), Taiwan, Republic of China, and Department of Metals and Materials Engineering, University of British Columbia, 309-6350 Stores Road, Vancouver, BC, V6T 1Z4, Canada

Received January 6, 2004; Revised Manuscript Received February 5, 2004

ABSTRACT

Nanoscale structural and mechanical characterization of the shell of a red abalone has been carried out. Cobble-like polygonal nanograins are basic building blocks that are used to construct individual aragonite platelets into a mother-of-pearl configuration known as nacre. The nanograin-structured aragonite platelets are not brittle in nature, but somewhat ductile. The deformability of the aragonite platelets together with the crack deflection, aragonite platelet slip, and organic adhesive interlayer contribute to the nacre's fracture toughness. Cracks formed in the outer prismatic layer of the shell do not show the crack diversion mechanism.

Nature has evolved highly complex and elegant mechanisms for materials design and synthesis.[1,2] Living organisms produce materials with physical properties that still surpass those of analogous synthetic materials with similar phase compositions.[2,4] Nature has long been using the bottom-up nanofabrication method to form self-assembled nanomaterials that are much stronger and tougher than many man-made materials formed top-down. Nacre (mother-of-pearl) is the best example of a bottom-up fabricated natural nanocomposite material that exhibits structural robustness, despite the brittle nature of its constituents. This material is composed of about 95% inorganic aragonite (a mineral form of $CaCO_3$), with only a few percent of organic biopolymer.[5] This ceramic/polymer composite material is of an extraordinary beauty, is well structured, and has high quality mechanical properties. Its laminated structure achieves approximately a two-fold increase in strength and a 1000-fold increase in toughness (work of fracture) over its constituent materials.[2] Such remarkable properties have inspired chemists and materials scientists to develop synthetic, biomimetic nanocomposite assemblies that attempt to reproduce nature's achievements.[6] The current techniques for synthesis are not very practical, though, because the micro/nanoarchitectures and toughening mechanisms of seashells have not been well explored or understood. This deficiency limits the potential for further development and improvement of biomimetic materials.

Structural characterization of nacre has mainly centered on the analysis of aragonite platelet crystal structure and lamellar microarchitecture. Little is known about the formation mechanisms of individual aragonite platelets. Nanoscale asperities were recently found on aragonite platelet surfaces.[5] The formation mechanisms of these nanoscale asperities are still unknown. Therefore, nanoscale structural characterization of individual aragonite platelets is needed for an in-depth understanding of the mechanisms at work within nacre.

Macroscopic beam-bending tests have been extensively used to study the resistance of nacre to catastrophic fracture, and several fracture models have been proposed based on the results of these analyses.[3−5] However, fabrication of a notch bend test specimen for fracture toughness measurement destroys the designed interaction between the aragonite platelets and makes it impossible to fully understand the functionality and mechanical integrity. The micro/nanoscale deformation and fracture mechanisms of nacre's structure are still not well understood. Detailed studies of the deformation behavior and the crack initiation and propagation

* Corresponding author. lixiao@engr.sc.edu.
† University of South Carolina.
‡ Chung Yuan Christian University.
§ University of British Columbia.

10.1021/nl049962k CCC: $27.50
Published on Web 02/27/2004

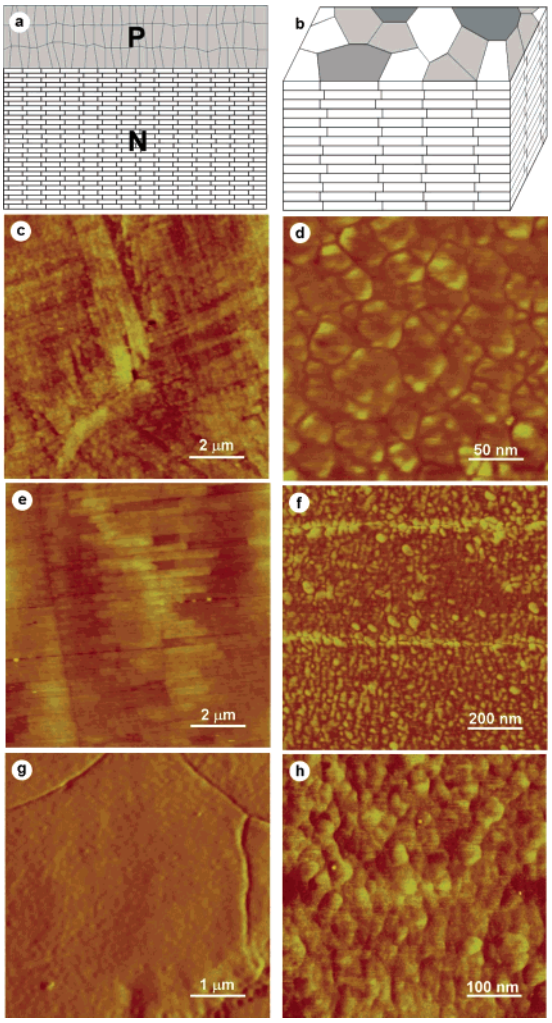

Figure 1. Micro/nanoarchitecture of the shell of a red abalone. (a) A schematic illustration of the crossed microarchitecture, including the prismatic (P) and nacreous (N) sections. (b) A schematic illustration of the nacreous section. Polygonal aragonite platelets are adhered into a lamellar structure by a thin organic interlayer. (c) and (d) AFM images of the prismatic section. The high magnification AFM phase image (d) shows nanograins within a prismatic column. (e) and (f) AFM images of the nacreous section. The high magnification AFM phase image (f) shows nanograins within an aragonite platelet. (g) and (h) AFM images of the nacre section that was prepared by cutting the shell along the shell plane. The existence of nanograins within individual aragonite platelets is affirmed by the high magnification AFM phase image (h).

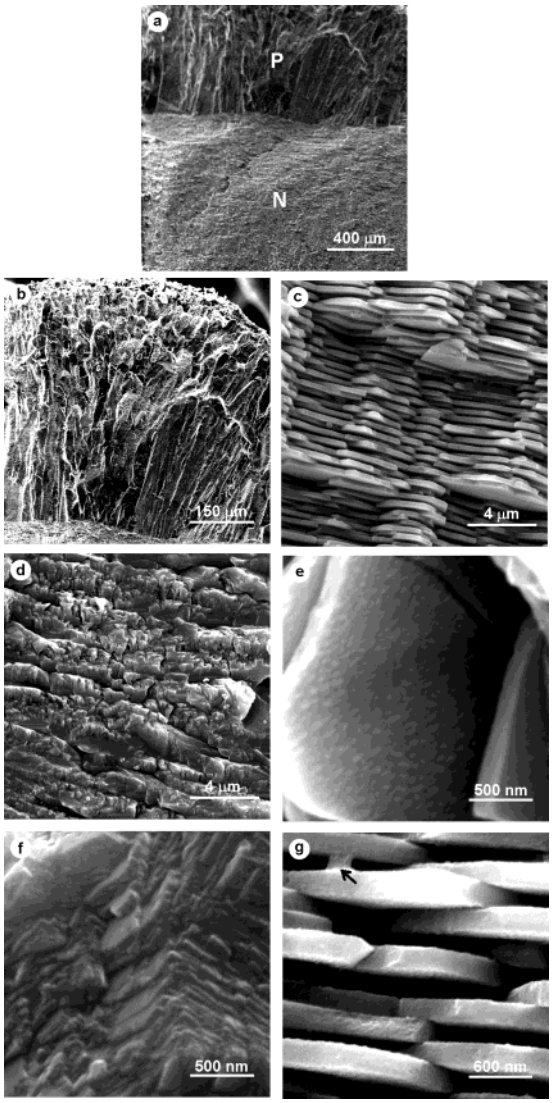

Figure 2. SEM images of the fracture shell surface. (a) Low magnification image showing the prismatic and nacreous regions. (b), (d), and (f) SEM images of the fracture surface of the prismatic section taken at increasing magnification. The prismatic section exhibits columnar architecture with cleavage fracture characteristics. (c), (e), and (g) SEM images of the nacreous section taken at increasing magnification. The brick mortar architecture is shown in (c). Nanoscale asperities on the aragonite platelet surface are readily observed in (e). The organic biopolymer is found to serve as adhesive to hold aragonite platelets, as indicated by arrow in (g).

mechanisms at the micro/nanoscale level combined with the structural characterization will help us understand how nature designs, synthesizes, and optimizes materials to achieve superior performance.

In this study, the nanoscale structure of red abalone shells was characterized using an atomic force microscope (AFM) and a scanning electron microscope (SEM). Hardness and elastic moduli were measured using a nanoindenter. Micro/nanocracks were generated using a microindenter in order to study the deformation and fracture mechanisms at the micro/nanoscale. From these investigations, deformation and fracture mechanisms are discussed in conjunction with architecture, hardness, elastic modulus, and energy-dissipation during cracking.

This study involves testing and analysis performed on shell specimens from California red abalone (Haliotis rufescens), which belongs to the class of gastropoda. The shells were collected alive in Santa Barbara, CA. To minimize the detrimental effect of drying on the structure and mechanical properties, they were cleaned and air-delivered in ice to the laboratory where the experiments were conducted. The specimens were sectioned by using a water-cooled, low-speed diamond saw. They were mechanically ground and polished using abrasives and powders down to 50 nm in size and rinsed thoroughly with distilled water prior to testing.

AFM observations were made with a Veeco Dimension 3100 AFM system (Veeco Metrology Group). Nano-

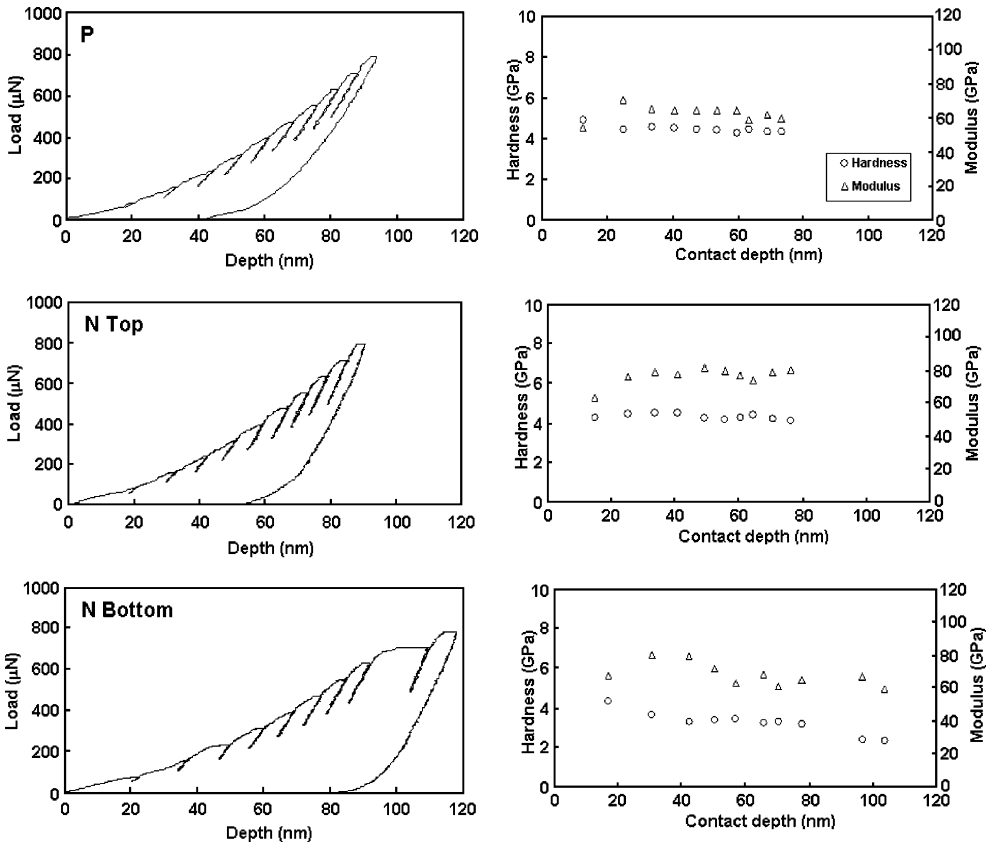

Figure 3. Multiple partial loading/unloading nanoindentations made on the polished abalone sample. The hardness and elastic modulus values were calculated from the load-displacement curves using standard techniques.

indentation tests were performed using a Troboscope nanomechanical testing system (Hysitron Inc.) in conjunction with the Veeco system. The Hysitron nanoindenter monitors and records the load and displacement of the indenter, a diamond Berkovich three-sided pyramid, with a force resolution of about 50 nN and displacement resolution of about 0.1 nm. Hardness and elastic moduli were calculated from the recorded load-displacement curves. The indentation impressions were then imaged using the Veeco AFM.

A microhardness tester with a diamond Vickers four-sided pyramid indenter was used to create cracks in the polished shell samples. The indentations were made with a normal load of 10 N held for 15 s. The indentation impressions and associated cracks were examined using a Nomarski optical microscope and the Veeco AFM.

Fractured shell samples were observed using a Philips XL30 field-emission environmental SEM.

The abalone shell has two microarchitecturally different regions, as shown in Figure 1. The outer region has the prismatic (P) section in which the calcitic (rhombohedral $CaCO_3$: *R*3*m*) crystallites are oriented perpendicular to the shell plane. The calcite crystallines are about a few micrometers in edge and have an aspect ratio of about 5.[7] AFM images (Figures 1c and 1d) show that each individual prismatic column consists of many nanometer-sized grains with a diameter of about 32 nm. The inner region has the nacreous (N) section; polygonal platelets of aragonite (orthorhombic, *Pmmm*) are oriented parallel to the shell plane to form close-packed confluent layers.[7] The aragonite platelets of a thickness of about 400 nm and an edge length of about 5 μm are separated by a 5−20 nm thick organic biopolymer interlayer, such that the cross section resembles a brick wall (Figure 1e). Polygonal platelets from neighboring layers overlap in such a manner that the interplatelet boundaries form tessellated bands perpendicular to the shell plane. Significant work has been performed on the crystallographic and morphological characteristics of the nacreous section.[5,7−9] However, nanoscale structural details within individual aragonite platelets have not been well understood. Previous transmission electron microscopy (TEM) studies showed that the electron diffraction pattern of individual aragonite platelets has the characteristic of single-crystal electron diffraction. This indicates that an aragonite platelet can be either a single crystal or a platelet of polycrystallines, with many small grains having the same crystal orientation. Although previously reported TEM bright-field images showed contrast with nanoscale grain characteristics,[8,9] such contrast might result from the ion milling process during TEM sample preparation. To date, conclusions have not been made due to lack of direct evidence. In the present study, cobble-like polygonal nanometer-sized grains with a diameter of about 32 nm were found within individual aragonite platelets using AFM, as shown in Figures 1e and 1f. Such nanograins were also found on the sample that was prepared by cutting the shell along the shell plane, as shown in Figures 1g and 1h. This affirms that a single aragonite platelet consists of a large amount of nanograins. It is believed that during biomineralization nanoparticles aggregate into indi-

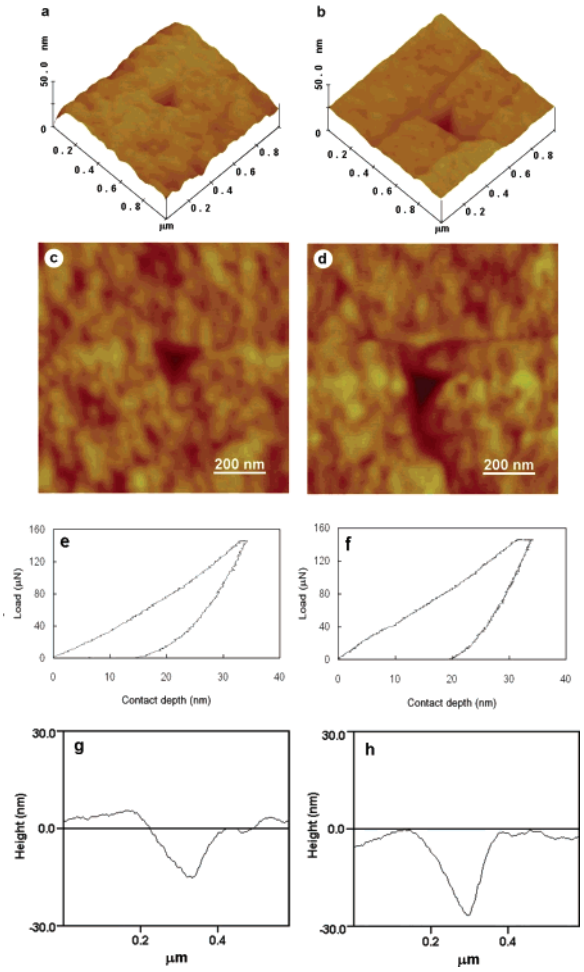

Figure 4. AFM images of nanoindentation marks on the (a and c) prismatic and (b and d) nacreous sections. Examination of area surrounding the indentation revealed no crack formation at the corners of the mark. Representative load-displacement curves for the (e) prismatic and (f) nacreous sections. Cross-sectional view of the indents for the (g) prismatic and (h) nacreous sections.

vidual platelets, and these nanoparticles are stacked along the same crystal orientation in the individual platelets to achieve extremely high adhesion.

Determination of the shell microstructure was also made from observations of the fractured shell specimen. Figure 2 shows SEM images of the cross section of a shell fragment that was broken in bending. Progressive magnification of the sample reveals that the prismatic section exhibits columnar architecture with cleavage fracture characteristics, while the nacreous section shows a clear brick−mortar organization. Nanoscale asperities were found on the aragonite platelet surfaces, as shown in Figure 2e. The size of these asperities is about 100 nm. One asperity consists of two or three surface nanograins that are used to form a surface peak−the asperity, as shown in Figure 1f. The organic biopolymer was found to serve as adhesive to hold aragonite platelets (Figure 2g). This is believed to be one of the major contributions to nacre's fracture toughness. This organic biopolymer consists of water-soluble and -insoluble material, mainly polysaccharide and protein layers. The polysaccharide matrix functions as the framework for insoluble proteins.[10]

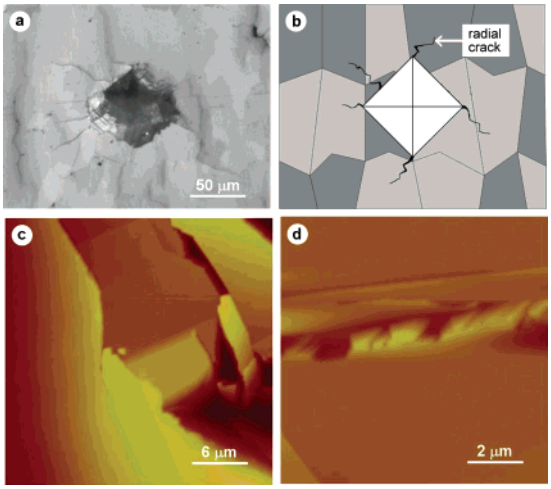

Figure 5. Images and schematic diagram of the fracture mechanics of the prismatic section. (a) Optical microscope image of a microindentation mark and (b) the corresponding schematic diagram. (c) and (d) AFM images of indentation radial cracks showing that the crack growth proceeded in a relatively unimpeded manner.

Multiple partial loading/unloading nanoindentations made on the polished abalone sample were used to determine the hardness and elastic modulus of the shell in each section as a function of depth. The data collected in the tests are displayed in Figure 3, along with hardness and elastic modulus values that were calculated from the load-displacement curves using standard techniques.[11−13] The hardness and elastic modulus values of the prismatic and nacreous sections are comparable. The variation in hardness and elastic modulus in the nacreous region is attributed to the interaction of the indenter with the organic biopolymer interlayers. It is interesting to note that the bottom part of the nacreous section exhibits slightly lower hardness and elastic modulus. Representative indentation marks on the prismatic and nacreous sections shown in Figure 4 show the pile-up resulting from the indentation, indicating plastic deformation. No cracks were found around the indent.

Indentations made with the microindenter were performed to produce micro/nanocracks in the polished shell sample. Optical microscope and AFM observations of the crack propagations shown in Figures 5 and 6 provide insight into the shell architecture. The prismatic section is brittle with radial cracks emanating from the indentation corners (Figures 5a and 5b). The AFM images of the indentation radial cracks (Figures 5c and 5d) show that the crack growth proceeded in a relatively unimpeded manner. This resulted in a lower fracture toughness for the outer region. The brittle outer region likely serves as a protective shield from piercing of the shell due to predaceous attacks from a sharp-clawed crustacean. The nacreous section shows structural robustness with short radial cracks emanating from the two indentation corners that are parallel to the shell plane, and an array of slip-bands along the other two indentation corners, as shown in Figure 6. The radial cracks initiated and propagated along the organic biopolymer interlayers in a zigzag manner. These cracks deflected from one platelet to another platelet as the crack growth proceeded. It has been long thought that nacre

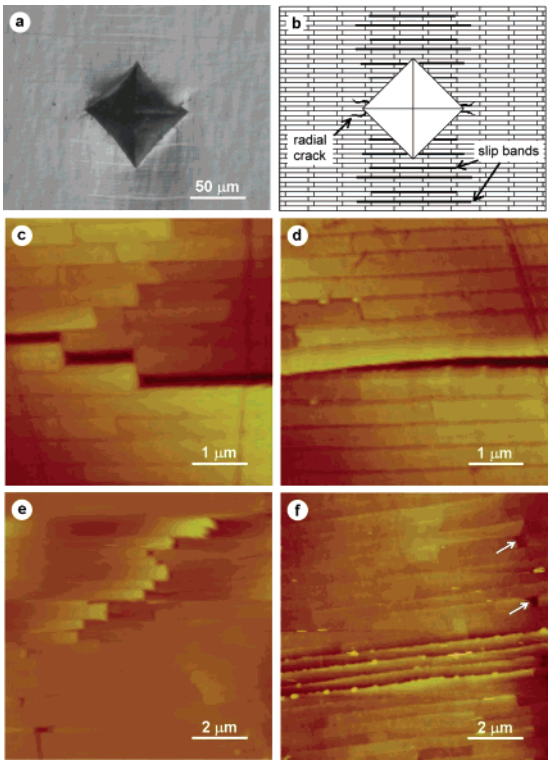

Figure 6. Images and schematic diagram of the fracture mechanics of the nacreous section. (a) Optical microscope image of a microindentation mark and (b) the corresponding schematic diagram. (c)−(e) AFM images of indentation radial cracks. (c) Crack deflection. (d) The deformed aragonite platelets at a crack tip. (e) Crack extrusion. (f) AFM image of a slip band and separations at platelet terminations, indicated by arrows.

aragonite platelets are brittle single crystals and cannot be plastically deformed. One of the interesting findings is that the aragonite platelets around the crack tip were plastically deformed during the crack propagation, indicating that aragonite platelets are not brittle in nature but somewhat ductile. This finding will change our conventional concept about aragonite platelets that they are brittle in nature. This plastic deformation allows the material to redistribute stress around strain concentration sites, thereby eliminating stress concentration and, consequently, blunting the crack tip. It is believed that the discovered ductility of aragonite platelets results from a large number of nanograins within the aragonite platelets.

During the crack deflection, the platelets around the crack extruded (Figure 6e), indicating slip between the platelets. This slip siphoned the crack energy and constrained the damage to a small volume around the crack. The most intriguing example is the array of slip-bands, as shown in Figure 6f. No radial cracks were found at the two indentation corners along the direction that is perpendicular to the shell plane. In each slip band three or four aragonite platelets slipped relative to each other. This made the polished cross section uneven with squeeze-in and squeeze-out of the platelets. Nanoscale particles were squeezed out at the platelet interfaces. These nanoparticles came from the platelet surface asperities that locked the adjacent platelets against their motion.[5] Between the slip bands separations at platelet terminations were observed, as indicated by arrows in Figure 6f. It is believed that the separations result from the interface rupture at the platelet edges. The separations opened as the adjacent interfaces slipped. The nanoscale asperities on the platelet surfaces can lock the neighboring platelets, thereby resisting the separations.

In summary, the abalone shell is a highly organized nanocomposite material designed to be extraordinarily tough while remaining hard and strong. In the nacreous layer, cobble-like polygonal nanograins are basic building blocks that are used to construct individual aragonite platelets. The nanograin-structured aragonite platelets are not brittle in nature, but somewhat ductile. The deformability of aragonite platelets together with the crack deflection, aragonite platelet slip, and organic adhesive interlayer result in a 1000-fold increase in toughness over its constituent materials. The outer prismatic layer did not show these crack diversion mechanisms and serves mainly as a brittle outer shield.

Acknowledgment. Financial support for this study was provided by the National Science Foundation (Contract No. EPS-0296165) and the University of South Carolina Nano-Center Seed Grant. Financial support for W.C.C.'s study leave was provided by the National Science Centre in Taiwan (92MEW0592JFD5001). The content of this information does not necessary reflect the position or policy of the Government and no official endorsement should be inferred.

References

(1) Li, X.; Nardi, P. *Nanotechnology* **2004**, *15*, 211−217.
(2) Rubner, M. *Nature* **2003**, *423*, 925−926.
(3) Kamat, S.; Su, X.; Ballarini, R.; Heuer, A. H. *Nature* **2000**, *405*, 1036−1040.
(4) Kessler, H.; Ballarini, R.; Mullen, R. L.; Kuhn, L. T.; Heuer, A. H. *Comput. Mater. Sci.* **1998**, *5*, 157−166.
(5) Wang, R. Z.; Sou, Z.; Evans, A. G.; Yao, N.; Askay, I. A. *J. Mater. Res.* **2001**, *16*, 2485−2493.
(6) Sellinger, A.; Weiss, P. M.; Nguyen, A.; Lu, Y. F.; Assink, R. A.; Gong, W. L.; Brinker, C. J. *Nature* **1998**, *394*, 256−260.
(7) Graham, T.; Sarikaya, M. *Mater. Sci. Eng. C* **2000**, *11*, 145−153.
(8) Feng, Q. L.; Cui, F. Z.; Pu, G.; Wang, R. Z.; Li, H. D. *Mater. Sci. Eng. C* **2000**, *11*, 19−25.
(9) Song, F.; Zhang, X. H.; Bai, Y. L. *J. Mater. Res.* **2002**, *17*, 1567−1570.
(10) Weiss, I. M.; Renner, C.; Strigl, M. G.; Fritz, M. *Chem. Mater.* **2002**, *14*, 3252−3259.
(11) Oliver, W. C.; Pharr, G. M. *J. Mater. Res.* **1992**, *7*, 1564−1583.
(12) Li, X.; Bhushan, B. *Mater. Charact.* **2002**, *48*, 11−36.
(13) Bhushan, B.; Li, X. *Int. Mater. Rev.* **2003**, *48*, 125−164.

NL049962K